Indian Journal of Science and Technology Vol. 5 No. 7 (July 2012) ISSN: 0974- 6846

Luminescence studies of Eu^{3+} doped $BaGd_2O_4$ phosphor

M. Srinivas* and B. Appa Rao
Department of Physics, Osmania University, Hyderabad-500 007, India
msrinivas.ou@gmail.com

Abstract

The spectroscopic properties of $BaGd_{2-x}O_4:Eu_x$ (x = 0.0 - 0.1) phosphors were investigated. The phosphors were synthesized by conventional solid state reaction method. The samples were characterized by powder-XRD and energy dispersive spectroscopy (EDS) techniques. The photoluminescence (PL) and thermally stimulated luminescence (TSL) studies of these materials were investigated. For PL studies the samples were excited with 258 nm UV light. All the samples showed strong red emission at 611 nm due to $^5D_0 \rightarrow {}^7F_2$ electric dipole transition of Eu^{3+} ions. PL peak intensity was found to increase with increase in the dopant concentration. For TSL studies, samples were γ-irradiated with different dose rates using ^{60}Co source. TSL of these phosphors showed a sharp glow peak with maxima at 394 K. Incorporation of europium activator in $BaGd_2O_4$ phosphor resulted in the increase of peak intensity. The trap parameters viz., order of kinetics (b), activation energy (E) and frequency factor (S) associated with the most intensive glow peak of $BaGd_2O_4:Eu^{3+}$ phosphor were determined using glow curve shape (Chen's) method. These phosphors can be useful in TL dosimetry

Keywords: Phosphors, Photoluminescence, U.V Excitation, Thermoluminescence, Dosimetry

Introduction

Rare earth-based phosphors are the most important trichromatic luminescent materials, with which full-color display is produced by emissions in the blue, green and red regions, respectively, at 450, 550 and 610 nm. The green and red emissions originate from the f-f transitions of Tb^{3+} and Eu^{3+} while the blue emission originates from the f-d transition of Eu^{2+}. For general lighting, photoluminescent materials including borates, silicates, aluminates, aluminoborates, aluminosilicates, nitrides, oxides etc., play very important role for the potential applications in ultraviolet devices. For example, in ultraviolet light emitting diode (UV LED) it is necessary to combine a UV chip with red, green, and blue (RGB) phosphors to generate white lights.

The luminescence of rare earth ions doped phosphors has been considerably interesting because of their applications in various types of display panels such as field emission display (FED) and plasma display panels (PDPs) (Ko *et al*., 2003; Jung & Seo, 2006; Lai *et al*., 2006; Kang & Liu, 2007). To achieve better resolution in these displays, it is important to develop phosphors with high quantum efficiency, controlled morphology and small particle size (Hsu *et al*., 2003). Sulfide-based phosphors represent one kind of important phosphor, but there are many problems with them (Jean-Charles Souriau *et al*., 2000; Nemec & Maly, 2000; Bol & Meijerink, 2000). When they are irradiated with an electron beam, they may cause decomposition and generate harmful gases, such as SO_2. Finally, the cathode exacerbates and the luminous efficiency of phosphors decreases. Recent studies have indicated that SrY_2O_4: Eu^{3+} is one of the promising red phosphor for FED applications (Yoshihiro *et al*., 2006); SrY_2O_4 and $BaGd_2O_4$ belong to the ordered $CaFe_2O_4$ structures (Brixner, 1967; Manivannan *et al*., 2003; JCPDS No. 42-1496). The aim of this work is to report the synthesis, photoluminescence (PL) and thermoluminescence (TL) of the $BaGd_2O_4$: Eu^{3+} phosphor. An analysis of the observed intensity-temperature TL data by making use of the glow curve shape (Chen's) method to determine the trapping parameters of this phosphor is presented and a plausible mechanism is discussed.

Experimental design

Materials of different compositions of $BaGd_{2-x}Eu_xO_4$ (x = 0.00, 0.02, 0.06 and 0.1) were synthesized by the conventional solid state reaction method. Stoichiometric amounts of $BaCO_3$, Gd_2O_3 and Eu_2O_3 (AR grade chemicals) were thoroughly mixed and ground together with ethanol in an agate mortar for 5 hours to give homogeneous mixture. The resultant powders were initially dried at 80^0C for 1 hour and heated in alumina boat at 1250^0C in air for 3 hours and subsequently allowed to cool down to room temperature.

Powder X-ray diffractograms were recorded on Philips X'pert Analytical X-ray diffractometer using Nickel filtered Cu-Kα radiation of wave length 1.5406 A^0 in the 2θ range of 10 ~ 80^0 with a step size of 0.04^0/ sec. The operating voltage and current of the instrument were maintained at 40 kV and 30 mA respectively. The compositions of the samples were obtained from their energy dispersive spectra (EDS). The EDS was attached to the HITACHI S-3700N model SEM instrument. The photoluminescence emission spectra were carried out using a Jobin Yvon-Spex Spectrofluorometer (Fluorolog version-3; Model FL3-11). The excitation source was a xenon arc lamp. The TSL studies were performed using PC based Thermoluminescence Analyzer system (type 1007) supplied by Nucleonix Systems Private Ltd., Hyderabad, India. The glow curves were recorded by heating the sample at a uniform rate of 2 K Sec^{-1} with the help of a temperature controller. All the measurements were performed at room temperature.

Indian Journal of Science and Technology Vol. 5 No. 7 (July 2012) ISSN: 0974- 6846

Results and discussion

Powder XRD

Fig.1. Powder XRD pattern of $BaGd_{1.9}Eu_{0.1}O_4$

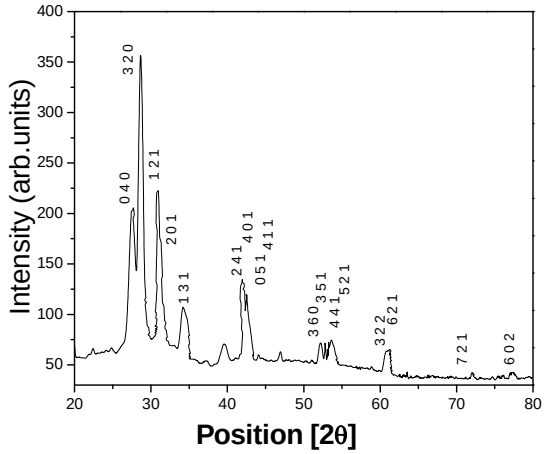

A typical powder X-ray diffractogram of $BaGd_{1.9}Eu_{0.1}O_4$ is shown in Fig.1. The diffractograms for other samples are similar with slight changes in the d-spacing. All the observed d-lines were indexed and the unit cell parameters were calculated using least square fit of powder XRD patterns. The "a", "b" and "c" values obtained for all the compounds are very close to that of reported values for $BaGd_2O_4$ (JCPDS No. 42-1496) confirming its orthorhombic structure at room temperature. The small deviations observed in lattice parameters of doped samples could be due to the difference in ionic size of Gd^{3+} and Eu^{3+}.

Energy dispersive Spectra (EDS)

The energy dispersive spectrum of 0.1 mole fraction of Eu^{3+} doped $BaGd_2O_4$ sample is shown in Fig.2. The peaks in the energy dispersive spectra confirm the presence of Ba, Gd, Eu and O in the $BaGd_2O_4$ powders.

Photoluminescence

Fig.3 (a) shows the excitation spectrum of $BaGd_2O_4$:Eu^{3+} was monitored at 611 nm. It shows broad bands with the maximum at about 258 nm, which can be attributed to the charge transfer state (CTS) this is related to the excitation of an electron from the oxygen 2p state to a Eu^{3+} 4f state (Blasse & Brill, 1967; Kubota *et al.*, 1998). The peaks situated at 277 nm and 314 nm, can be attributed to the $^8S_{7/2} \rightarrow {}^6I_{7/2}$ and $^8S_{7/2} \rightarrow {}^6P_{7/2}$ transitions of Gd^{3+} respectively, which indicates that the efficient energy transfer from Gd^{3+} to Eu^{3+} (Pires *et al.*, 2002).

The emission spectra of $BaGd_2O_4$:Eu^{3+} by exciting at 258 nm is shown in Fig 3 (b). Upon excitation with 258 nm under UV excitation, the emission spectrum was described by the well known $^5D_0$ level to ^7F_J (J = 0, 1, 2, 3) line emissions of the Eu^{3+} ions are located around 581, 586, 591, 598, 611, 628, 651 and 661 nm. The most intense line at 611 nm corresponds to the hypersensitive

Fig.2. EDS spectra of $BaGd_{1.9}Eu_{0.1}O_4$

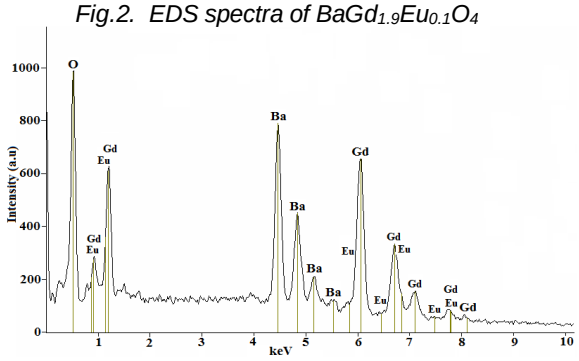

Fig.3 (a and b) Excitation and Emission spectra of $BaGd_{1.9}Eu_{0.1}O_4$

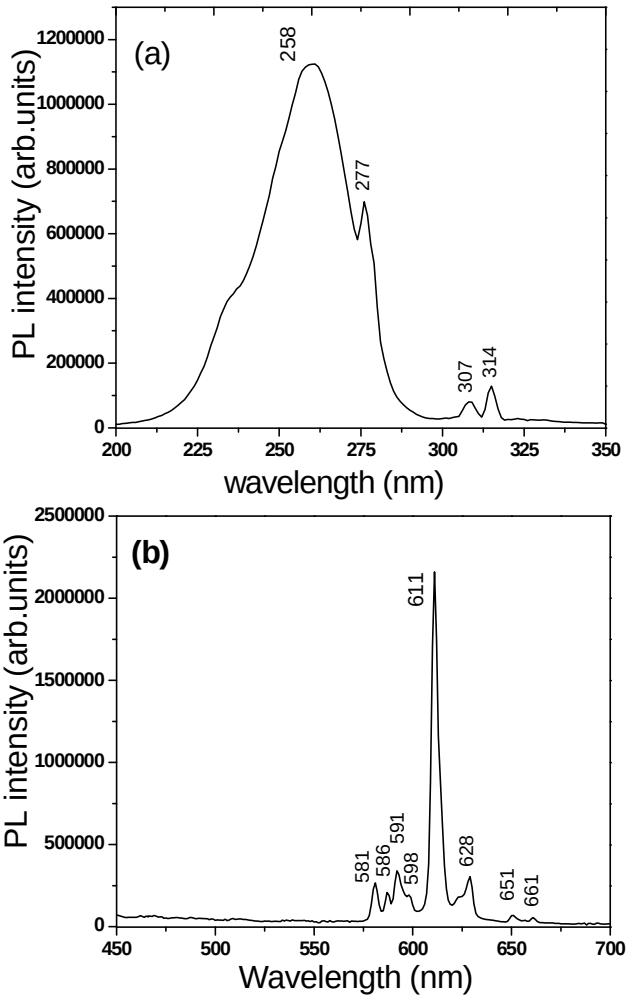

transition between the $^5D_0$ and ^7F_J level of Eu^{3+} ion, which is electric dipole forbidden and sensitive to the ligand environment (Shionoya & Yen, 1999). In PL emission we have observed that the luminescence intensity increased with the increasing Eu^{3+} concentration. The effect of Eu^{3+} content in $BaGd_2O_4$ on the relative photoluminescence

Indian Journal of Science and Technology Vol. 5 No. 7 (July 2012) ISSN: 0974- 6846

Fig.4. Emission spectra of $BaGd_2O_4$: Eu

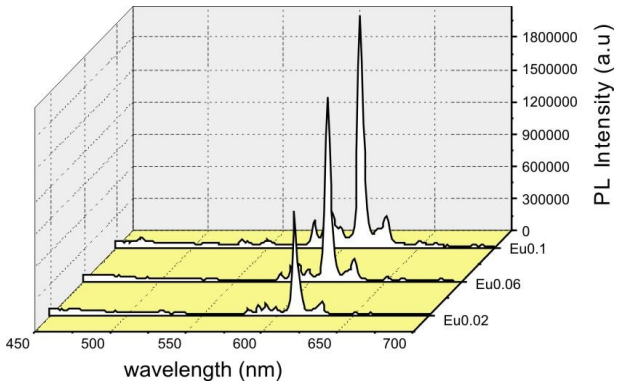

Fig.5. TSL glow curves of $BaGd_2O_4$: Eu with 1520 Gy dose

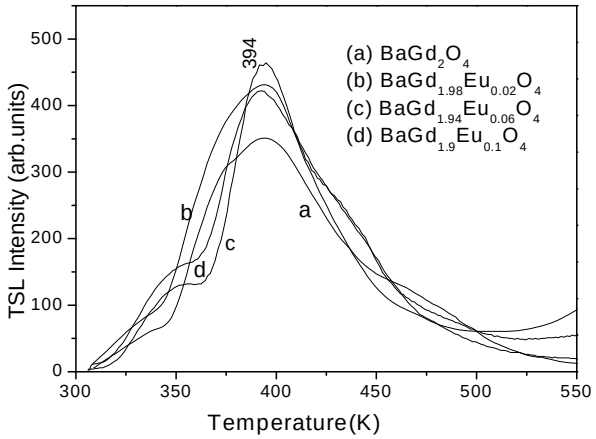

Fig.6. The variation of TL light output of $BaGd_2O_4$ phosphor with the concentration of Eu^{3+} irradiated with different γ-ray doses.

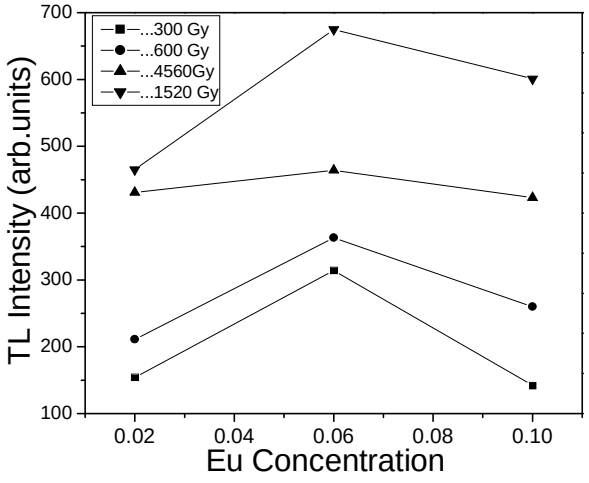

intensity at 611 nm is shown in Fig.4. The highest photoluminescence intensity was found at a doped-Eu^{3+} concentration of 0.1 mol fraction. The crystallographic structures of $BaGd_2O_4$ have been investigated (Taibi *et al.*, 1994; Yoshihiro *et al.*, 2006). It has been reported that the rare earth occupies two point sites allowed in the structure (C_s symmetry) with the trivalent europium as local probe (LIDE, 2002). The radius of Ba^{2+} is 0.135 nm, Eu^{3+} is 0.095 nm (coordination number = 6) and Gd^{3+} is 0.094 nm. Due to the different valence states and difference of the ion sizes between Ba^{2+} and Eu^{3+}, we can conclude that the Eu^{3+} ions substitute Gd^{3+} sites rather than Ba^{2+} sites. Usually, the splitting into number of the states ^7F_J (J = 0, 1, 2, 3 and 4) of Eu^{3+} depends on the J value with the maximum of 2J+1 and the site symmetry (Chuai *et al.*, 2002). Therefore the phosphor may be useful for all display devices as red emission phosphor.

Thermoluminescence

In order to study the effect of dopant concentration on glow curves, the thermally stimulated luminescence (TSL) signals were measured. During this study, glow curves of Eu doped $BaGd_2O_4$ samples were recorded for different dose rates of γ-irradiation (300, 600, 1520 and 4560 Gy). Glow curves of the Eu^{3+} doped phosphor recorded for 1520 Gy shown in Fig. 5. A strong TSL glow peak is observed at 394 K. It is observed that the intensity of this glow peak is found to increase with the increase of Eu^{3+} concentration up to x = 0.06 and then decreases for higher concentration i.e., for x = 0.1. It is also observed that glow peak intensity increases with dose rate up to 1520 Gy and decreases for 4560 Gy. The strong TSL glow peak indicate that a set of traps are being activated within the particular temperature range each with its own value of activation energy (E) and frequency factor (S).

The Fig.6 shows a comparison of intensities of the glow peaks, the addition of Eu impurity to undoped $BaGd_2O_4$ compound enhances the TL intensity. This shows that Eu^{3+} impurity is a suitable dopant for $BaGd_2O_4$ compound for enhancement of the TSL response. Decrease in the TL light output has been observed with higher Eu^{3+} concentration (x = 0.1) and higher dosage indicates that there may be some saturation in the TL output at this dose of irradiation and concentration.

It has been suggested that the glow curves of Eu^{3+} doped $BaGd_2O_4$ is related to the relaxation of the excited Eu^+ ions $(Eu^+)^*$. Upon irradiation, Eu^+ ions either trap an electron to become Eu^0 or they trap a hole to become Eu^{++} ions:

$$Eu^+ + \text{electron} \rightarrow Eu^0$$
$$Eu^+ + \text{hole} \rightarrow Eu^{++}$$

On thermal stimulation, these europium atom/ions give rise to TSL emission according to the following mechanism

$$Eu^0 + \text{hole} \rightarrow (Eu^+)^* \rightarrow Eu^+ + h\nu \text{ or}$$
$$Eu^{++} + \text{electron} \rightarrow (Eu^+)^* \rightarrow Eu^+ + h\nu$$

In general, the undoped sample, whose emission can be related to intrinsic defects or to some unwanted impurity in the starting powder, exhibits a poor TL efficiency than the doped samples. In such cases, TSL response is found to be insufficient for reliable studies in

Indian Journal of Science and Technology Vol. 5 No. 7 (July 2012) ISSN: 0974- 6846

Table 1. Trap parameters of $BaGd_2O_4:Eu^{3+}$

Sample	Dose(Gy)	T_m (K)	μ_g	Activation Energy (eV)				S (Sec^{-1})
				E_τ	E_δ	E_ω	E_{av}	
$BaGd_2O_4$	300	394	0.5	0.675	0.718	0.700	0.698	8.43×10^7
$BaGd_{1.98}Eu_{0.02}O_4$	300	394	0.573	0.671	0.650	0.659	0.660	2.61×10^7
$BaGd_{1.94}Eu_{0.06}O_4$	300	394	0.645	0.871	0.686	0.746	0.768	7.43×10^8
$BaGd_{1.90}Eu_{0.10}O_4$	300	394	0.706	0.983	0.930	0.722	0.778	1.02×10^9
$BaGd_2O_4$	600	395	0.611	0.685	0.613	0.638	0.645	1.57×10^7
$BaGd_{1.98}Eu_{0.02}O_4$	600	395	0.571	0.723	0.694	0.707	0.708	1.17×10^8
$BaGd_{1.94}Eu_{0.06}O_4$	600	394	0.640	0.903	0.718	0.780	0.800	2.02×10^9
$BaGd_{1.90}Eu_{0.10}O_4$	600	394	0.573	0.861	0.800	0.827	0.829	4.94×10^9
$BaGd_2O_4$	1520	394	0.604	0.701	0.633	0.658	0.644	2.98×10^7
$BaGd_{1.98}Eu_{0.02}O_4$	1520	394	0.585	0.769	0.711	0.735	0.738	3.00×10^8
$BaGd_{1.94}Eu_{0.06}O_4$	1520	394	0.658	0.925	0.697	0.768	0.796	1.80×10^9
$BaGd_{1.90}Eu_{0.10}O_4$	1520	394	0.686	1.003	0.684	0.775	0.821	3.79×10^9
$BaGd_2O_4$	4560	393	0.623	0.715	0.616	0.650	0.661	2.82×10^7
$BaGd_{1.98}Eu_{0.02}O_4$	4560	394	0.671	1.030	0.735	0.824	0.863	1.39×10^{10}
$BaGd_{1.94}Eu_{0.06}O_4$	4560	394	0.707	1.130	0.707	0.819	0.885	2.79×10^{10}
$BaGd_{1.90}Eu_{0.10}O_4$	4560	394	0.688	1.104	0.739	0.843	0.895	3.77×10^{10}

the low dose range measurements. On the other hand, as expected, the TL signal steadily increased after incorporation of Eu impurities, which are well known as efficient activators in many materials. In the present study it is observed that the glow curve shapes of undoped and Eu doped samples are different indicating that there are interactions between intrinsic defects and doped impurities.

Trap parameters: Trap parameters such as order of kinetics (b), activation energy (E) and frequency factor (S) were calculated for the 394 K glow peak of $BaGd_2O_4$:Eu phosphor using the Chen's method (Chen *et al*., 1997; Nagabhushana *et al*., 2008).

Glow curve peak shape method: Using the peak shape method**,** the shape parameters of the present samples namely the total half intensity width ($\omega = T_2 - T_1$), the high temperature half width ($\delta = T_2 - T_m$) and the low temperature half width ($\tau = T_m - T_1$), where T_m is the peak temperature and T_1 and T_2 are temperature on either side of T_m corresponding to half peak intensity were determined and are presented in Table1.

Order of kinetics: To determine the order of kinetics, the form factor or symmetry factor (μ_g) which uses the known values of shape parameters was calculated by using the following equation

$$\mu_g = \frac{\delta}{\omega} = \frac{T_2 - T_m}{T_2 - T_1}$$

The evaluated symmetry factor of the present samples was given in Table 1. Theoretically, the form factor that ranges between 0.42 and 0.52 is close to 0.42 for first order kinetics and 0.52 for second order kinetics. The average value of μ_g in the present study was found to be 0.62 which suggest that this peak obeys second order kinetics.

Activation energy: Activation energy (*E*) was calculated (Chen's method) using the formula

$$E_\alpha = c_\alpha \left(\frac{k T_m^2}{\alpha}\right) - b_\alpha (2 k T_m)$$

Where α = τ, δ and ω with $\tau = T_m - T_1$, $\delta = T_2 - T_m$ and $\omega = T_2 - T_1$

$c_\tau = 1.51 + 3.0(\mu_g - 0.42)$, $b_\tau = 1.58 + 4.2(\mu_g - 0.42)$

$c_\delta = 0.976 + 7.3(\mu_g - 0.42)$, $b_\delta = 0$

$c_\omega = 2.52 + 10.2(\mu_g - 0.42)$, $b_\omega = 1$.

Where $\mu_g = \frac{\tau}{\delta}$

Frequency factor: Once the order of kinetics and activation energy were determined, the frequency factor (S) can be calculated from the following equation (Nagabhushana *et al*., 2008)

$$\frac{\beta E}{k T_m^2} = S \exp\left(-\frac{E}{k T_m}\right)\left[1 + (b-1)\Delta_m\right]$$

Where $\Delta_m = 2kT_m/E$, b is the order of kinetics, *k* the Boltzmann constant (8.6×10^{-5} eV K^{-1}) and β is the linear heating rate (2 K Sec^{-1}). The kinetic parameters of $BaGd_2O_4:Eu^{3+}$ phosphor materials in the present study are given in Table-1.

From the data, it is obvious that a considerable amount of retrapping takes place in all second-order peaks. It is believed that there are some deep and shallow traps and for this reason there could be retrapping of the electrons at deep traps going to upper shallow traps by stimulation due to thermal energy. The competition among them might be giving various releasing and retrapping probabilities, which might have resulted in different frequency factors. The traps could be either electron traps or hole traps or of both kinds (Salah *et al*., 2004). However, it should be mentioned that this point needs more detailed investigations using other techniques such as thermostimulated conductivity, TL emission, electron spin resonance, photoluminescence, photoacoustic studies/optical absorption, etc., in order to understand the TL mechanism, trapping and

Indian Journal of Science and Technology Vol. 5 No. 7 (July 2012) ISSN: 0974- 6846

recombination centers associated with thermostimulated light emission of Eu^{3+} doped barium gadolinium oxide phosphor.

Conclusions

XRD study confirms that the Eu^{3+} doped $BaGd_2O_4$ compound has orthorhombic structure at room temperature. The EDS studies confirm the formation of $BaGd_2O_4$: Eu^{3+} phosphor. The PL spectra show the strongest emission at 611 nm corresponds to the electric dipole $^5D_0 \rightarrow {}^7F_2$ transition of Eu^{3+}, which results in emission of pure red color. The TL sensitivity of pure $BaGd_2O_4$ phosphor is enhanced with the incorporation of Eu^{3+} impurity. Hence, these phosphors can be useful in TL dosimetry. The phosphor $BaGd_2O_4$: Eu^{3+} is found to have second-order kinetics in TSL studies. The values of trapping parameters of the 394 K glow peak of these phosphors calculated by Chen's method yields a very good agreement between the trapping parameters.

Acknowledgement

The author wishes to thank Dr. M.T. Jose and U.Madhusoodanan IGCAR, Kalpakkam, for providing photoluminescence and thermoluminescence facility and also acknowledges the UGC, New Delhi, for a research fellowship under FIP programme.

References

1. Kang CC and Liu RS (2007) The effect of terbium concentration on the luminescent properties of yttrium oxysulfide phosphor for FED application, *J. Lumin*. pp: 122-123, pp: 574-576.
2. Ko MG, Park JC, Kim DK and Byeon SH (2003) Low-voltage cathodoluminescence property of Li-doped $Gd_{2-x}Y_xO_3$: Eu^{3+}. *J. Lumin*. 104, 215-221.
3. Lai Hh, Chen Bj, Xu W, Xie Yh, Wang Xj and Di WH (2006) Fine particles $(Y,Gd)P_xV_{1-x}O_4$: Eu^{3+} phosphor for PDP prepared by co-precipitation reaction, *Mater. Lett*. 60, 1341-1343.
4. Jung HK and Seo KS (2006) Luminescent properties of Eu^{2+}-activated $(Ba, Sr)_3MgSi_2O_8$ phosphor under VUV irradiation, *Opt. Mater*. 28, 602-605.
5. Hsu WT, Wu WH and Lu CH (2003) Synthesis and luminescent properties of nano-sized $Y_3Al_5O_{12}$: Eu^{3+} phosphors, *Mater. Sci. Engg.* B104, 40-44.
6. Jean-Charles Souriau, Yong Dong Jiang, John Penczek, Henry Paris G and Christopher Summers J (2000) Cathodoluminescent properties of coated $SrGa_2S_4$:Eu^{2+} and ZnS:Ag,Cl phosphors for field emission display applications *Mater. Sci. Engg.* B76, 165-168.
7. Nemec P and Maly P (2000) Temperature study of trap-related photoluminescence decay in CdS_xSe_{1-x} nanocrystals in glass, *J. Appl. Phys*. 87, 3342.
8. Bol AA and Meijerink A (2000) Doped semiconductor nanoparticles - a new class of luminescent materials? *J. Lumin*. 87, 315-318.
9. Yoshihiro D, Wataru N and Yukio H (2006) Crystal structures and magnetic properties of magnetically frustrated systems $BaLn_2O_4$ and $Ba_3Ln_4O_9$ (Ln = lanthanide), *J. Phys. Condens. Matter.* 18, 333-344.
10. Manivannan V, Comanzo HA, Setlur AA, Srivastava AM, Schmidt PA and Happek U (2003) Nature of luminescent centers in Cerium activated materials with the $CaFe_2O_4$ structure, *J. Lumin*. pp: 102-103, pp: 635-637.
11. Brixner LH (1967) Fluorescence and Cathodoluminescence of Eu^{3+} in Some alkali and alkaline earths-yttrates and gadolinates as hosts. *J. Electrochem. Soc. Solid State Sci.* 114, 252-254. JCPDS No. 42-1496.
12. Kubota S, Suzuyama Y, Yamane H and Shimada M (1998) Luminescence properties of $LiSr_2Y_{1-x}Ln_xO_4$ (Ln=Eu,Tb,Tm) ($0 \le x \le 1$) *J. Alloys Compd*. 268, 66-71.
13. Blasse G and Brill A (1967) Fluorescence of Eu^{3+}-Activated Lanthanide Oxyhalides *J. Chem. Phys*. 46, 2579-2582.
14. Pires AM, Santos MF, Davolos MR and Stucchi EB (2002) The effect of Eu^{3+} ion doping concentration in Gd_2O_3 fine spherical particles. *J. Alloys Compd.* 344, 276-279.
15. Shionoya S and Yen WM (1999) Phosphor handbook CRC Press, Boca raton. pp: 190.
16. Taibi M, Aride J, Antic-Fidancev E and Lemaitre-Blaise M (1994) Etude de la fluorescence de Eu^{3+} dans $BaRE_2O_4$ (RE = Gd, Y). Détermination des paramètres du champ cristallin. *Phys. Status Solid.* A144, 453-459.
17. LIDE D (2002) Editor in chief, the CRC handbook of Chemistry and Phys. On CD-ROM, CRC Press, Version. 22.
18. Chuai XH, Zhang HJ, Sh Li F, Sh Z Lu, J Lin, Sh B Wang and Chou KC (2002) Synthesis and luminescence properties of oxyapatite $NaY_9Si_6O_{26}$ doped with Eu^{3+}, Tb^{3+}, Dy^{3+} and Pb^{2+}. *J.Alloys Compd.* 334, 211-218.
19. Chen R and Mc Keever SWS (1997) Theory of thermoluminescence and related phenomenon. *World Scientific Singapore*. pp: 29.